Title

Astrocyte structural reactivity and plasticity in models of retinal detachment

Authors

Luna, Gabriel
Keeley, Patrick W
Reese, Benjamin E
et al.

Publication Date

2016-09-01

DOI

10.1016/j.exer.2016.03.027

Peer reviewed

HHS Public Access

Author manuscript

Exp Eye Res. Author manuscript; available in PMC 2017 September 01.

Published in final edited form as:

Exp Eye Res. 2016 September ; 150: 4–21. doi:10.1016/j.exer.2016.03.027.

Astrocyte Structural Reactivity and Plasticity in Models of Retinal Detachment

Gabriel Luna[1,2], **Patrick W. Keeley**[1], **Benjamin E. Reese**[1,4], **Kenneth A. Linberg**[1], **Geoffrey P. Lewis**[1,2], and **Steven K. Fisher**[1,2,3]

[1]Neuroscience Research Institute, University of California Santa Barbara

[2]Center for Bio-Image Informatics, University of California Santa Barbara

[3]Department of Molecular, Cellular and Developmental Biology, University of California Santa Barbara

[4]Department of Psychological and Brain Sciences, University of California Santa Barbara

Abstract

Although retinal neurodegenerative conditions such as age-related macular degeneration, glaucoma, diabetic retinopathy, retinitis pigmentosa, and retinal detachment have different etiologies and pathological characteristics, they also have many responses in common at the cellular level, including neural and glial remodeling. Structural changes in Müller cells, the large radial glia of the retina in retinal disease and injury have been well described, that of the retinal astrocytes remains less so. Using modern imaging technology to describe the structural remodeling of retinal astrocytes after retinal detachment is the focus of this paper. We present both a review of critical literature as well as novel work focusing on the responses of astrocytes following rhegmatogenous and serous retinal detachment. The mouse presents a convenient model system in which to study astrocyte reactivity since the Müller cell response is muted in comparison to other species thereby allowing better visualization of the astrocytes. We also show data from rat, cat, squirrel, and human retina demonstrating similarities and differences across species. Our data from immunolabeling and dye-filling experiments demonstrate previously undescribed morphological characteristics of normal astrocytes and changes induced by detachment. Astrocytes not only upregulate GFAP, but structurally remodel, becoming increasingly irregular in appearance, and often penetrating deep into neural retina. Understanding these responses, their consequences, and what drives them may prove to be an important component in improving visual outcome in a variety of therapeutic situations. Our data further supports the concept that astrocytes are important players in the retina's overall response to injury and disease.

Correspondance: Steven K. Fisher, Ph.D., Neuroscience Research Institute, University of California Santa Barbara, Santa Barbara, CA 93106-5060. steven.k.fisher@lifesci.ucsb.edu. Phone: (805)-893-3637. Fax: (805)-893-2005.

Keywords

glia; astrocyte; retinal astrocytes; astrocyte reactivity; astrocyte hypertophy astrocyte remodeling; astrocyte structural plasticity; retinal detachment

Introduction

Retinal astrocytes, are generally not considered particularly reactive cells when compared to the large radial Müller glia (Fisher and Lewis, 2003; Fisher et al., 2005; Reichenbach and Bringmann, 2013; Smith et al., 1997; Vogler et al., 2014). Indeed, since their first descriptions by neuroanatomists such as Ramón y Cajal, Golgi, Virchow, and Deiters in the mid-19th century, the exact functionality of astrocytes in the central nervous system (CNS) has been controversial. These cells were initially referred to as “connective tissue” or as their name implies, “nerve glue” (Kettenmann and Verkhratsky, 2008; Somjen, 1988). However, as technology has improved, more precise descriptions of their roles have emerged: i.e., their functional roles in development, synaptic function and plasticity, the blood-brain/retina barrier, injury responses, learning, memory, and even the regulation of breathing (Chung et al., 2013; Fields et al., 2014; Gourine et al., 2010; Pearson-Leary et al., 2015). However, fundamental questions remain such as whether astrocytes within a defined region of the CNS comprise a homogenous population (Zhang and Barres, 2010). One of the best-studied features of brain and spinal cord astrocytes is their “reactivity” following injury or in neurodegenerative disease or injury, including the prominent formation of “glial scars” (Buffo et al., 2010; Pekny and Pekna, 2014; Sofroniew, 2009). However questions remain about the exact roles and mechanisms of action in this well-described situation. Reactivity by retinal astrocytes has received less attention because of the more obvious responsiveness of the larger Müller cells (Charteris et al., 2002; Eibl et al., 2007; Erickson et al., 1983; Sethi et al., 2005). Simple PubMed searches with key phrases “astrocytes, brain and/or spinal cord injury” or “astrocytes and retinal injury” return 641 references for the former and 245 for the latter between 1975 and 2016. Comparatively, the much smaller retinal astrocytes with their very fine processes, have proven more difficult to study. There is, however, recent data indicating that optic nerve head (ONH) astrocytes undergo important structural remodeling in glaucoma and optic nerve crush (Lye-Barthel et al., 2013; Sun and Jakobs, 2012; Sun et al., 2010). Here we provide a study of the normal structure of astrocytes in a variety of species and show that they undergo significant remodeling after retinal detachment, thus providing further evidence that the reactivity of these cells is worthy of additional study.

Studies in the uninjured cerebral cortex and hippocampus demonstrate that protoplasmic astrocytes anatomically tile, each occupying distinct spatial domains that do not change size in response to injury (Ogata and Kosaka, 2002; Wilhelmsson et al., 2006). Our data suggest that the tiling or overlap of retinal astrocytes as well as their structural responses to retinal injury may be more difficult to categorize.

Unlike retinal neurons, astrocytes do not seem to form a class of cell that systematically varies across the retina. Their morphology can vary greatly among adjacent cells, with few easily observable patterns in spatial positioning, length, branching or the overlap of their

processes. It thus has proven difficult to determine if there is heterogeneity or systematic varation in this cell population. Jammalamadaka and colleagues (Jammalamadaka et al., 2015) recently demonstrated that astrocytes vary morphologically, based on their association with either superficial veins or arteries on a whole-tissue scale. Such spatial metrics are an essential step in determining potential heterogeneity in the population, and whether, for instance, networks exist among possible sub-types or whether their morphology can be associated with specific functional properties.

In the normal retina, astrocytes label more heavily with anti-glial fibrillary acidic protein (GFAP) than the Müller cell endfeet (which predominately express the type-III intermediate filament, vimentin), but after injury there is a rapid up-regulation of GFAP by Müller cells. In comparison to many species, however, the Müller cell response in the mouse retina is relatively muted, permitting better visualization of the astrocytic response. Hence, most of the data presented here will focus on induced and spontaneous retinal detachment in the mouse retina as a model that allows for the systematic study of these cells.

Methods

This study was conducted in accordance with the National Institutes of Health *Guide for the Care and Use of Laboratory Animals*, the Association and Accreditation of Laboratory Animal Care International (AAALAC) guidelines, and under the authorization of the Institutional Animal Care and Use Committee at the University of California Santa Barbara. Animals were placed on a standard rodent diet *ad libitum* and housed under a 12h/12h light-dark cycle.

Induced Retinal Detachments

Retinal detachment surgery varied among species and can be found in detail elsewhere (Lewis et al., 1999; Linberg et al., 2002; Luna et al., 2010; Verardo et al., 2008). In short, retinal detachments were created in right eyes using a pre-pulled glass pipette with an inside diameter of 30μm (World Precision Instruments, Sarasota, FL). A small incision was made below the level of the lens for the insertion of the pipette and then a solution of 0.25% sodium hyaluronate (Healon, Pharmacia, Piscataway, NJ) was infused between the retina and underlying retinal pigmented epithelium to prevent the retina from reattaching. However, in ground squirrel retinas balanced salt solution (BSS, Alcon Inc., Ft. Worth, TX) was used to allow for subsequent reattachment.

Spontaneous Retinal Detachments: Generation of nm3342 mice

Data from the nm3342 mutant mice used in this study were obtained in collaboration with Dr. Sheldon S. Miller (National Eye Institute, Bethesda, MD). The original description and generation of the strain are described elsewhere (Chang et al., 2008a). In these animals a spontaneous “serous” type detachment forms without tearing of the retinal tissue and leakage of vitreous beneath the neural retina, as occurs in rhegmatogenous detachments.

Antibodies and Immunofluorescence for Mouse Retinal Wholemounts

To create retinal wholemounts, normal (*Mus musculus*) and mutant mice eyes were immersion fixed overnight in 4% paraformaldehyde in 0.1M sodium cacodylate buffer (pH: 7.4), after which the retina was dissected free from the RPE. Four incisions were made in the retina to allow the wholemounted retina to lie flat on a slide in a characteristic “iron cross” shape (Stone, 1981). The wholemounts were then rinsed in phosphate buffered saline (PBS; pH 7.4) 3 × 15 mins. and 1 × 60 mins., and subsequently immersed in normal donkey serum 1:20 in PBS containing 0.5% BSA, 0.1% Trition-X 100, and 0.1% sodium azide (PBTA) at 4°C on a rotator for continuous overnight agitation. Wholemounts were incubated in primary antibodies to label astrocyes, blood vessels, and ganglion cell bodies and their axons: GFAP conjugated to Cy3 (1:100, mouse monoclonal, Sigma-Aldrich, St. Louis, MO), collagen IV (1:250, goat polyclonal, Millipore, Temecula, CA), and SMI-32 (1:200, mouse monoclonal, Covance, San Diego, CA), respectively. They were then rinsed in PBTA at which time donkey anti-goat-647 and anti-mouse-488 antibodies (Jackson ImmunoResearch Laboratories; West Grove, PA) diluted 1:200 in PBTA were added overnight at 4°C. Finally, the secondary antibodies were rinsed and retinal wholemounts were mounted using Vectashield (Vector Laboratories, Inc; Burlingame, CA) on a glass slide and sealed under an 18 × 18 #0 micro coverslip (Thomas Scientific; Swedesboro, NJ) using nail polish.

Single Cell Injections

Dye-injections in lightly fixed tissue (i.e., 30 mins. in 4% buffered paraformaldehyde) were carried out as described elsewhere (Keeley and Reese, 2010). After preparing the wholemounts as above, retinas were stained with the nuclear stain Hoechst 33342 (Invitrogen; Carlsbad, CA) diluted 1:1000 in PBS for 1 hour, rinsed with PBS, then transferred to a fixed stage Nikon Eclipse E600 epifluorescence microscope (Nikon Instruments Inc., Melville, NY). Using a 60× water dipping objective lens, single astrocyte cell bodies were identified based on Hoechst staining and position in the most vitreal layer of the retina, and then impaled with a micropipette filled with 5% Lucifer yellow (LY) or Alexa Fluor 568 (AF) (Invitrogen; Carlsbad, CA) and iontophoretically filled with a negative current of approximately 5nA. In some cases retinas were subjected to antibody staining following single cell injections.

Mosaic Acquisition and Image Registration

Recent advances in microscopy as well as computer science have provided the means to optically capture large-scale, wide-field datasets of biological specimens using both light and electron microscopy (Anderson et al., 2009; Chow et al., 2006). These techniques allow for a more precise qualitative and computational analysis of targeted tissues while avoiding the problems inherent in tissue sampling to study specific cell types. These advances have necessitated and spurred the development of tools for data storage, access, viewing, annotation, and analysis (Anderson et al., 2011; Martone et al., 2008). Here we use modifications of these advances to describe astrocytes of the entire murine retina, avoiding the pitfalls of regional sampling.

Specimens were viewed and imaged using an Olympus Fluoview 1000 laser scanning confocal microscope (Center Valley, PA) equipped with an argon 488nm photodiode laser,

HeNe 543/633 photodiode lasers, UPlanFLN 40x oil immersion lens N.A. 1.30, as well as a precision motorized stage (Applied Scientific Instrumentation, Inc. Eugene, OR). Optical sections were sampled between 1–0.5 μm intervals in the z-direction using a 1024 × 1024 pixel array in the x–y axis. Image stacks were collected sequentially using the Olympus Fluoview software version 2.1a. To generate large scale, high-resolution montages, images were collected with a 20% overlap among individual tiles. The registration technique is based on the automatic detection of feature points; the estimation of the transformation is obtained using robust estimators on the putative matches obtained matching the intensities of the point neighborhoods. In order to ensure high quality results containing the maximum amount of original unchanged data blended without blur and abrupt intensity differences, a blending technique is employed by using a robust algorithm to adjust the photometric appearance of the images in overlapping regions, whereby individual seams are automatically identified and fused across image tiles. Resultant datasets were then assembled using the bio-image software *Imago* 1.5 (Mayachitra Inc; Santa Barbara, CA).

Results

Murine Retina

Comparing the anti-GFAP staining of control and experimentally detached retinas in high-resolution, wide-field wholemounts provides an overview of the astrocyte population and changes the cells undergo after detachment (Fig. 1). Because each high-resolution montage consists of approximantely 400 seamlessly aligned and registered z-projected images (Fig. 1A, F), one can examine in detail any selected region of the entire montage, thus giving both a global overview and a high-resolution view of local areas of interest within the retina (Fig. 1E, J). This also includes the ability to rotate z-stacks from a selected tile to provide an orthogonal view of the cells. In the normal mouse retina, the generalized description of astrocytes as having a slender stellate morphology (Figs. 1B–E) with prominent branches making discrete endfoot-like contacts on BVs applies most specifically to those cells whose cell bodies do not directly appose BVs (Fig. 1C, examples indicated by asterisks). As will be shown, these cells also make contact on each other, blood vessels, ganglion cells, and axons After four months of sustained retinal detachment, these astrocytes show robust anti-GFAP staining, and a more diffuse, “ragged” and irregular appearance (Figs. 1G–J), particularly at their terminal endings which appear to acquire many fine filopodial-like terminations (Figs. 1I, J). In some areas of the montages these astrocytes underlying a detachment appear to be entangled and overlapping rather than maintaining a more tiled, discrete appearance. Although it is difficult to make exact determinations in the wholemounts because it is impractical to collect image data through the depth of the retina from the vitreal to photoreceptor sides, data from retinal cross-sections clearly show a correlation between a detached region and changes in astrocyte morphology (data not shown). Thus an area showing the changes in astrocyte morphology can be reliably associated with an area of photoreceptor degeneration induced by the detachment. A major question is how information about an injury at the photoreceptor/RPE interface is transmitted to cells that lie on the opposite side of the retina. It is possible that molecules released by damaged photoreceptors diffuse across the retina. However, it is well-established that the effects of photoreceptor degeneration are transmitted to 2nd and 3rd order neurons as well as Müller

cells, thus also forming a potential indirect cell-to-cell pathway (Coblentz et al., 2003; Fariss et al., 2000; Humayun et al., 1999; Iandiev et al., 2008; Strettoi et al., 2002).

Anti-GFAP labels only the IF component of the cells' cytoplasm leaving the potential for unseen morphology. Images of LY injected astrocytes along with antibody labeling provide the best method for observing both the complete morphology of single cells and their interactions (Fig. 2). They also clearly show differences in cells that lie in the space between BVs (Figs. 2A–D, F, G) and those whose cell bodies appear to directly appose a specific BV (i.e., "perivascular," Fig. 2E). The labeling of isolated cells by dye-filling demonstrates that the branched stellate cells terminate with a more discrete "endfoot" which itself can vary from a club-like ending to a larger more flattened area of contact (Figs. 2A–D; arrows). These cells were often observed to extend a single long process that contacts a distant BV (Fig. 2F). The perivascular cells tend to have more of an ensheathing relationship to the contacted BV (Fig. 2E). These data further support the conclusion of dividing astrocytes into at least two morphologically-based populations with implications of functional differences (Zahs and Wu, 2001). The stellate (intravascular) cells form contacts between different BVs, other astrocytes, and ganglion cell bodies as well as their axons, thus forming a cellular "intermediary network" for the maintence of neurons. It seems more likely that the perivascular cells play some role in maintaining or regulating the cells of the BV with which they associate.

After injecting adjacent individual cells with two different intracellular dyes, the astrocytes can be described as having both tiling (Figs. 3A–C) and overlapping relationships (Figs. 3D–F), the former being similar to that of protoplasmic astrocytes found in grey matter (Bushong et al., 2002) (Inset, Fig. 3B, 3C). Interestingly, astrocytes that display more overlapping of their processes are almost exclusively of the perivascular type, and these cells seem to stain more heavily with anti-GFAP. While the intravascular tiling astrocyte population in detached retina shows distinctive morphological remodeling, data from dye-filed cells suggest that they do not dramatically change their overall relationship with neighboring astrocytes (Figs. 3F, G).

The 3D renderings created from dye-filled cells demonstrate the very planar nature of the stellate astrocytes (Fig. 3H and inset; red), especially when compared to that of the large radial Müller cells (Fig. 3H, green). Figure 3H also shows that a single astrocyte covers a large area on the retinal surface by comparison to the area covered by the endfeet of a single Müller cell.

The combined data from dye-injected cells and immunolabeling experiments demonstrate three distinct properties of astrocytes. (1) They extend no more than 10μm into the retina (i.e. in the z-dimension) under normal conditions (Fig. 3H). (2) In addition to showing terminal endings on BVs and other astrocytes (Figs. 3A, B; arrows in B), they also contact cell bodies in the ganglion cell layer (Figs. 4A–D; arrows), ganglion cell axons (Figs. 4E–H; arrows in E and H) and display a close relationship with Müller cells (Fig. 3H, arrows). (3) The stellate astrocytes have the ability to cover large areas of the retinal surface with their extensive branches (Fig. 3H, red) by comparison to endfoot branches of single Müller cells (Fig. 3H, inset, green). This evidence suggests that astrocytes must remodel during

development as these other cellular components (i.e. ganglion cells, and their axons, as well as Müller cell endfeet) develop later than the influx of astrocytes. Astrocytic processes commonly follow a relatively linear trajectory, thus giving most of the cells the classic "star-shaped" morphology (supplemental Figs. 2, 3). However, in some cases such as shown in figures 4E and F (arrow) they can curve dramatically apparently to contact ganglion cell axons bundles. In other cases, astrocytic processes extend across the retinal surface to ganglion cell axons and appear to contact the axon bundles with several smaller individual processes (Fig. 4H; arrows). The relationship between astrocytes and ganglion cell axons is much simpler in the mouse than in other species such as humans, cat, or ground squirrel.

Figure 5 shows a different data-set from normal and detached mouse retinas demonstrating the consistency of morphological changes between animals, i.e., a transition from a smooth, slender morphology in normal retina (Figs. 5A–C; green), to a thickened, disorganized appearance with extended "fan-like" terminals in detached retinas (Figs. 5D–F; green). Most commonly, astrocytes reacting to injury are described as "hypertrophic," although data from the dye-injected cells suggest strongly that the increased anti-GFAP staining remains within the general domain of the cells in normal retina, that is, the cells still generally occupy domains of about the same size on the retinal surface with little overlap of their processes.

The 3D reconstruction of astrocytes reveals an additional aspect of these cells' reaction to detachment, one that is difficult to observe and reliably document in single-section data, namely, the growth of processes into the retina. After 4 months of detachment the normally planar cells (Fig. 6A; red; normal retina) show both more "thickened" lateral processes on the retinal surface (Figs. 6B, C), and often have one or more processes extending into the inner plexiform layer, where they always branch adjacent to BVs (Figs. 6B, C; red, arrows). In some instances astrocytes extend processes as far as the outer plexiform layer, using BVs as an apparent scaffold (Figs. 6D, E; red, arrows). Reactive astrocytic processes were easily distinguishable from the thinner, more linear, GFAP-stained Müller cell radial processes (Figs. 6C, E; asterisks). The association between astrocytes and BV after retinal injury could have important physiological consequences. Indeed, in an animal model of Huntington's disease astrocytes promote angiogenesis and reduce the number of pericytes associated with BV by an increased production of vascular endotheial growth factor (A) and IkB (Hsiao et al., 2015)

We used data from the single dye-filled cells to probe for changes that may occur in single cells between normal and detached retinas. Figures 7A and B show projected images of nine LY dye-filled astrocytes from a normal mouse retina and from a retina detached for 2 months. Visually the astrocytes in Fig. 7B appear 'thickened' with fewer fine processes, thus encompassing the usual definition of "hypertrophy". However, when the surface area covered by the cells was determined by creating a convex polygon linking the furthest points for each cell (see Fig. 7A, upper left cell), cells from the attached and detached regions were not statistically different from one another (Fig. 7C). Similarly, there were no detectable changes between apparent somal areas of astrocytes in the two groups (Fig. 7D). Although no clearly quantifiable differences in size were apparent, these data were generated from 2-D projections of the cells and data from the 3D reconstructions of the immunolabeled cells show that the expansion of astrocyte processes into the retina is a common phenomenon

after detachment. In a normal dye-filled astrocyte discrete terminal processes are oberserved (Fig. 8A), however, after two months of retinal detachment terminal processes appear thinkened and display a frayed appearance (Fig. 8B). By rotating the astrocyte in figure 8A the highly planar nature of the cell in the normal retina is easily observed (Fig. 8C). However, when the cell is rotated in the same manner in the detached retina we observe conspicuous growth of processes into the retina among the population of single dye-filled cells (Figs. 8D, E).

Another newly appreciated feature of these cells' response to detachment is their reorganization within the optic nerve head (ONH). In the normal retina, ONH astrocytes display a slender and organized appearance (Fig. 9A) defining spaces for ganglion cell axons as they make their way into the optic nerve (Fig. 9B; asterisks). One month after a retinal detachment anti-GFAP staining reveals that the ONH astrocytes lose their sleek appearance, becoming disorganized (Fig. 9C) so that the glial openings are poorly defined and reduced in size (Fig. 9D, asterisks). This phenomenon is similar to what has been described in glaucomatous eyes where it has been proposed to be involved in the strangulation of ganglion cell axons and ultimate death of ganglion cells (Balaratnasingam et al., 2008; Nguyen et al., 2011; Son et al., 2010).

Astrocytes also become highly reactive in the mutant strain of mice that generate spontaneous serous retinal detachments (the *nm3342/RPE1a* mouse; (Chang et al., 2008b) similar to that found in POMGnT1-deficent mice (Takahashi et al., 2011) where detachments occcur with no retinal tear or break. In areas of attached retina in mutant animals, astrocytes display the stellate morphology found in normal murine retina (Fig. 10A). In areas underlying the spontaneous detachments, astrocytes undergo significant remodeling (Fig. 10B); even more vigourously than after rhegmatogenous detachment by increasing their expression of GFAP, by assuming a thicker more ragged appearance, by increasing their coverage of BV, and by sprouting thick processes into the inner retina (Fig. 10C, arrows; see supplemental movie).

Rat Retina

The response of the astrocytes after induced rhegmatogenous detachment in the Long Evans rat (*Rattus norvegicus*) essentially mirrors that of the murine retina. Normal astrocytes are relegated to the nerve fiber layer (NFL) and heavily express GFAP (Fig. 11A; green). After detachment they remodel alongside BVs as in mouse retina; interestingly, they also upregulate the expression of type-III intermediate filament protein, synemin (Figs. 11B–D; red, arrows), which is normally down-regulated in mature animals (Luna et al., 2010). Müller cells increase their expression of GFAP, but maintain their basic radial orientation within the retina (Fig. 11D; red, asterisks), showing no particular affinity for BVs as they expand within the retina and extend processes into the subretinal space (Lewis et al., 1995).

Human Retina

As in all other species studied, astrocytes in normal human retina display a slender and organized appearance ending in discrete terminal processes. They differ from astrocytes in rodents, because their processes form extensive tracks that run parallel to ganglion cell axon

bundles on the vitreal surface (Figs. 12A, B; green). In eyes affected by age-related macular degeneration, human astrocytes lose their linear organization and become a tangled web of processes among the axons in what may be similar to fibrotic scars that form elsewhere in the CNS (Figs. 12C, D; green).

Cat Retina

Astrocytes in the domestic cat retina (*Felis catus*) are similar to those in the human retina, forming well-defined linear tracks running coincident with ganglion cell axon bundles (Fig. 13A, B; green). These tracks appear hypertrophic within a week of experimental rhegmatogenous detachment becoming disorganized, seem more numerous in the GCL and intertwine with expanded Müller cell endfeet (Figs. 13C, D; arrows, green) (Lewis and Fisher, 2006).

Squirrel Retina

The astrocyte-Müller cell response in the cone-dominant California ground squirrel retina (*Otospermophilus beecheyi*) is different than that observed in all other species studied to date. In the normal retina, GFAP-labeled astrocytes form a very thin plane along the NFL (Figs. 14A, 14D; green). When the retina is detached for 1 day and reattached for 7, the astrocytes show profuse branching into the inner retina, sending long GFAP-positive processes to the outer limiting membrane (OLM) (Figs. 14B, C; green, arrows) with their processes running parallel to axon bundles. Unlike any other species, the radial Müller cells appear to remain quiescent, and do not show the typical up-regulation of GFAP expression. Interestingly, when examining astrocytes in wholemounted preparations they uncharacteristically lack a preferential affinity towards superficial BVs (Figs. 14D, E; green), instead it is the Müller cell endfeet that increase their contact with BVs after detachment (Fig. 14F; red).

Discussion

Astrocyte reactivity has long been a hallmark accompaniment to injury and neurodegeneration in the brain and spinal cord and a topic of study for many decades. It has not received as much attention in the retina, probably because there has not been a clear association between glial scar formation and axonal regeneration as is the case in the brain and spinal cord. The up-regulation and reorganization of the intermediate filament protein GFAP, a principal component of the cytoskeleton in glial cells has long been a key signature of astrocyte reactivity. The functional role for GFAP is poorly understood. It has generally been considered, along with vimentin to play a role in stabilizing the structure of glial cells and their expansion during hypertrophic reactivity. Indeed, in retinal detachment, the absence of GFAP expression results in a markedly muted response of glial cells, and leads to the increased preservation of photoreceptors (Nakazawa et al., 2007) through unknown mechanisms. In mice lacking the intermediate filaments GFAP and vimentin an increased neural integration into the retina from transplanted tissue grafts has also been demonstrated (Kinouchi et al., 2003), perhaps from a lack of formation of rigid glial scars. In the brain and spinal cord, astrocyte reactivity has been speculated as serving dual purposes: isolation of regions of degeneration by the formation of glial scars, thus sparing healthy tissue from the

detrimental effects of neurodegeneration, and secondly maintaining homeostasis of the extracellular environment (Bush et al., 1999). In light-damaged retinas, glial scars formed by Müller cells may form similar “seals” around regions of neurodegeneration (Marc et al., 1998), and their involvement in maintaining retinal homeostasis seems fairly clear from evidence in a variety of retinal degenerative conditions, including retinal detachment (Marc et al., 1998). There is also evidence that retinal astrocytes generate intracellular Ca^{+2} waves and their stimulation in rat retina can evoke dilation of neighboring arterioles (Srienc et al., 2012), thus supporting a functional linkage for the structural interaction between astrocytes and BV’s. The role of astrocyte reactivity in photoreceptor degenerative conditions, whether induced mechanically or genetically clearly shows their structural remodeling is a prominent response (Fernández-Sánchez et al., 2015; Karschin et al., 1986).

Once initiated neurodegeneration in the retina is irreversible. Indeed, most emerging therapies are aimed simply at arresting the process. Only recently has a specific role for astrocytes in this process received any attention. Astrocytes in the ONH have been implicated in elevated intraocular pressure and ganglion cell death in glaucoma (Cooper et al., 2015; Dai et al., 2012; Ju et al., 2015). Although the implications are not clear, here we show that there are similar structural changes in ONH astrocytes in response to retinal detachment. Detachment does lead to systematic remodeling of retinal ganglion cell dendrites so there may be some unknown functional link between these two events (Coblentz et al., 2003). The emerging data suggest that astrocytes are an important component in the overall response of the retina to various neurodegenerative conditions.

Astrocytes and Müller cells probably both contribute to a so-called proliferative disease of the retina, proliferative vitreoretinopathy (PVR) by the formation of glial scars. Immunocytochemical data show clearly the major role for Müller cells but also suggest the presence of astrocytes in the cellular membranes that form in the vitreous in PVR (Lesnik Oberstein et al., 2008; Oberstein et al., 2011). The proliferation and migration of these two cell types early in the formation of epiretinal membranes suggest that their reactivity may be primary events in the disease. PVR occurs in about 10% of successful reattachment surgeries; there are no preventive measures (Girard et al., 1994; Joeres et al., 2006; Kwon et al., 2016), and the only treatment is surgical removal of the cellular membranes. Thus understanding the mechanisms underlying glial reactivity has immediate implications for an important sight-threatening human disease. Studies in the “atypically reactive” ground squirrel may provide opportunities to examine the reactivity of astrocytes in the absence of the overwhelming response of Müller cells (Sakai et al., 2003).

The most prominent morphological phenotype of astrocyte is the stellate appearance of their processes, characteristic of fibrous astrocytes elsewhere in the CNS, with long processes reaching out to the BVs, ganglion cell bodies, axons, and other astrocytes. A second morphological type of GFAP-expressing astrocyte lies against and spreads along a single BV (Jammalamadaka et al., 2015; Zahs and Wu, 2001). There is still much to be learned about the function of retinal astrocytes in the normal retina and their role in various ocular diseases or injuries. They are known to proliferate in response to injury (Geller et al., 1995; Luna et al., 2010) and lose their regular array and stellate shape coincident with the expansion of Müller cell endfeet on the retinal surface (Lewis and Fisher, 2003), but whether there is an

interrelationship between the two is unknown. Studies in the ground squirrel do suggest that astrocyte reactivity can occur independently of typical Müller cell reactivity (Sakai et al., 2003). The data presented here demonstrate that the effect of retinal detachment on astrocytes is not trivial, resulting in significant changes in GFAP expression and overall remodeling of the cells' morphology. The exact physiological effects of these changes remain to be discovered. It is also not known if astrocytes recover their organization and morphology after long-term retinal reattachment. This could be an important step in the recovery of overall retinal homeostasis, since abnormal astrocytes may contribute to the breakdown of the blood-retinal barrier, thus altering the metabolic profile of the tissue (Chan-Ling and Stone, 1992).

The phenomenon of neuronal remodeling as a regular occurrence in retinal injury and disease only began to be appreciated in the late 1990s (Coblentz et al., 2003; Lewis et al., 1998; Marc et al., 1998; Strettoi and Pignatelli, 2000). Structural remodeling of Müller cells (gliosis) was appreciated long before (Erickson et al., 1987) and is now recognized as an important component of virtually all photoreceptor degenerative conditions (Rattner and Nathans, 2006; 2005). Our data and that from studies examining retinal and optic nerve head astrocytes demonstrate that these cells can now be added to the list of cells participating in this response (Sun and Jakobs, 2012).

The study of astrocyte morphology has largely occurred by immunocytochemical labeling with anti-GFAP, which labels only the IF component of the cells' cytoplasm, or about 15% of the total volume of a given cell (Bushong et al., 2002) creating the potential for unseen morphological changes. Employing a combination of anti-GFAP and cytoplasmic markers such as S100 or glutamine synthetase (GS) can reveal a more detailed delineation of an astrocytes' true morphology (Ghandour et al., 1983) but this approach, like anti-GFAP labeling also has an important limitation since there is virtually homogeneous staining of the whole population making it difficult to resolve individual cells and their interactions. Dye-filling is a more accurate and complete method for the study of individual cells, but it is labor-intensive, making it difficult to obtain data for a large population of cells (see supplemental figures 1, 2). The organization of cellular domains within biological systems is a common phenomenon (Bushong et al., 2004; Honda, 1983; Reese and Keeley, 2014; Senft and Woolsey, 1991) and the domain of dendritic arbors is commonly used to classify neuronal sub-types in the retina (Amthor and Oyster, 1995; Keeley and Reese, 2010; Wässle et al., 1981). Unlike retinal neurons, astrocyte morphology varies greatly with few easily observable patterns across the retina, thus it has proven difficult to determine if there is heterogeneity in the population that may be responsible for defining domains of different astrocytic types. The use of new technology such as the creation of a "Brainbow" mouse (Livet et al., 2007) that expresses a large variety of fluorescent markers in individual astrocytes could aid greatly in resolving issues about the astrocyte population and its responses to retinal injury or disease.

As new therapeutic approaches are being developed to preserve retinal structure, it seems reasonable to suggest that astrocytes, given their prominence in the retina, their intimate relationship with the vasculature and retinal ganglion cells and remodeling in the face of

photoreceptor degeneration, should be considered potentially important players in this process.

Supplementary Material

Refer to Web version on PubMed Central for supplementary material.

Acknowledgments

Support: National Science Foundation (IIS-0808772 and ITR-0331697). Macula Vision Research Foundation. Santa Barbara Cottage Hospital Research Grant. International Retinal Research Foundation. National Eye Institute (EY-019968).

References

Amthor FR, Oyster CW. Spatial organization of retinal information about the direction of image motion. Proc Natl Acad Sci USA. 1995; 92:4002–4005. [PubMed: 7732021]

Anderson JR, Jones BW, Yang JH, Shaw MV, Watt CB, Koshevoy P, Spaltenstein J, Jurrus E, UKV, Whitaker RT, Mastronarde D, Tasdizen T, Marc RE. A computational framework for ultrastructural mapping of neural circuitry. PLoS Biol. 2009; 7:e1000074.doi: 10.1371/journal.pbio.1000074 [PubMed: 19855814]

Anderson JR, Mohammed S, Grimm B, Jones BW, Koshevoy P, Tasdizen T, Whitaker R, Marc RE. The Viking viewer for connectomics: scalable multi-user annotation and summarization of large volume data sets. J Microsc. 2011; 241:13–28. DOI: 10.1111/j.1365-2818.2010.03402.x [PubMed: 21118201]

Balaratnasingam C, Morgan WH, Bass L, Ye L, McKnight C, Cringle SJ, Yu DY. Elevated pressure induced astrocyte damage in the optic nerve. Brain Res. 2008; 1244:142–154. DOI: 10.1016/j.brainres.2008.09.044 [PubMed: 18848926]

Buffo A, Rolando C, Ceruti S. Astrocytes in the damaged brain: molecular and cellular insights into their reactive response and healing potential. Biochem Pharmacol. 2010; 79:77–89. DOI: 10.1016/j.bcp.2009.09.014 [PubMed: 19765548]

Bush TG, Puvanachandra N, Horner CH, Polito A, Ostenfeld T, Svendsen CN, Mucke L, Johnson MH, Sofroniew MV. Leukocyte infiltration, neuronal degeneration, and neurite outgrowth after ablation of scar-forming, reactive astrocytes in adult transgenic mice. Neuron. 1999; 23:297–308. [PubMed: 10399936]

Bushong EA, Martone ME, Ellisman MH. Maturation of astrocyte morphology and the establishment of astrocyte domains during postnatal hippocampal development. Int J Dev Neurosci. 2004; 22:73–86. DOI: 10.1016/j.ijdevneu.2003.12.008 [PubMed: 15036382]

Bushong EA, Martone ME, Jones YZ, Ellisman MH. Protoplasmic astrocytes in CA1 stratum radiatum occupy separate anatomical domains. J Neurosci. 2002; 22:183–192. [PubMed: 11756501]

Chan-Ling T, Stone J. Degeneration of astrocytes in feline retinopathy of prematurity causes failure of the blood-retinal barrier. Invest Ophthalmol Vis Sci. 1992; 33:2148–2159. [PubMed: 1607225]

Chang B, Hawes NL, Hurd RE, Wang J. A New Mouse Model of a Retinal Detachment With Secondary Angle Closure Glaucoma. … & Visual Science. 2008a

Chang B, Hawes NL, Hurd RE, Wang J. A New Mouse Model of a Retinal Detachment With Secondary Angle Closure Glaucoma. … & Visual Science. 2008b

Charteris DG, Sethi CS, Lewis GP, Fisher SK. Proliferative vitreoretinopathy-developments in adjunctive treatment and retinal pathology. Eye (Lond). 2002; 16:369–374. DOI: 10.1038/sj.eye.6700194 [PubMed: 12101443]

Chow SK, Hakozaki H, Price DL, MacLean NAB, Deerinck TJ, Bouwer JC, Martone ME, Peltier ST, Ellisman MH. Automated microscopy system for mosaic acquisition and processing. J Microsc. 2006; 222:76–84. DOI: 10.1111/j.1365-2818.2006.01577.x [PubMed: 16774516]

Chung WS, Clarke LE, Wang GX, Stafford BK, Sher A, Chakraborty C, Joung J, Foo LC, Thompson A, Chen C, Smith SJ, Barres BA. Astrocytes mediate synapse elimination through MEGF10 and MERTK pathways. Nature. 2013; 504:394–400. DOI: 10.1038/nature12776 [PubMed: 24270812]

Coblentz FE, Radeke MJ, Lewis GP, Fisher SK. Evidence that ganglion cells react to retinal detachment. Exp Eye Res. 2003; 76:333–342. [PubMed: 12573662]

Cooper ML, Crish SD, Inman DM, Horner PJ, Calkins DJ. Early astrocyte redistribution in the optic nerve precedes axonopathy in the DBA/2J mouse model of glaucoma. Exp Eye Res. 2015; doi: 10.1016/j.exer.2015.11.016

Dai C, Khaw PT, Yin ZQ, Li D, Raisman G, Li Y. Structural basis of glaucoma: the fortified astrocytes of the optic nerve head are the target of raised intraocular pressure. Glia. 2012; 60:13–28. DOI: 10.1002/glia.21242 [PubMed: 21948238]

Eibl KH, Lewis GP, Betts K, Linberg KA, Gandorfer A, Kampik A, Fisher SK. The effect of alkylphosphocholines on intraretinal proliferation initiated by experimental retinal detachment. Invest Ophthalmol Vis Sci. 2007; 48:1305–1311. DOI: 10.1167/iovs.06-0591 [PubMed: 17325177]

Erickson PA, Fisher SK, Anderson DH, Stern WH, Borgula GA. Retinal detachment in the cat: the outer nuclear and outer plexiform layers. Invest Ophthalmol Vis Sci. 1983; 24:927–942. [PubMed: 6862796]

Erickson PA, Fisher SK, Guérin CJ, Anderson DH, Kaska DD. Glial fibrillary acidic protein increases in Müller cells after retinal detachment. Exp Eye Res. 1987; 44:37–48. [PubMed: 3549345]

Fariss RN, Li ZY, Milam AH. Abnormalities in rod photoreceptors, amacrine cells, and horizontal cells in human retinas with retinitis pigmentosa. Am J Ophthalmol. 2000; 129:215–223. [PubMed: 10682975]

Fernández-Sánchez L, Lax P, Campello L, Pinilla I, Cuenca N. Astrocytes and Müller Cell Alterations During Retinal Degeneration in a Transgenic Rat Model of Retinitis Pigmentosa. Front Cell Neurosci. 2015; 9:484.doi: 10.3389/fncel.2015.00484 [PubMed: 26733810]

Fields RD, Araque A, Johansen-Berg H, Lim SS, Lynch G, Nave KA, Nedergaard M, Perez R, Sejnowski T, Wake H. Glial biology in learning and cognition. Neuroscientist. 2014; 20:426–431. DOI: 10.1177/1073858413504465 [PubMed: 24122821]

Fisher SK, Lewis GP. Müller cell and neuronal remodeling in retinal detachment and reattachment and their potential consequences for visual recovery: a review and reconsideration of recent data. Vision Res. 2003; 43:887–897. [PubMed: 12668058]

Fisher SK, Lewis GP, Linberg KA, Verardo MR. Cellular remodeling in mammalian retina: results from studies of experimental retinal detachment. Prog Retin Eye Res. 2005; 24:395–431. DOI: 10.1016/j.preteyeres.2004.10.004 [PubMed: 15708835]

Geller SF, Lewis GP, Anderson DH, Fisher SK. Use of the MIB-1 antibody for detecting proliferating cells in the retina. Invest Ophthalmol Vis Sci. 1995; 36:737–744. [PubMed: 7890504]

Ghandour MS, Langley OK, Clos J. Immunohistochemical and biochemical approaches to the development of neuroglia in the CNS, with special reference to cerebellum. Int J Dev Neurosci. 1983; 1:411–425. DOI: 10.1016/0736-5748(83)90023-0 [PubMed: 24873695]

Girard P, Mimoun G, Karpouzas I, Montefiore G. Clinical risk factors for proliferative vitreoretinopathy after retinal detachment surgery. Retina (Philadelphia, Pa). 1994; 14:417–424.

Gourine AV, Kasymov V, Marina N, Tang F, Figueiredo MF, Lane S, Teschemacher AG, Spyer KM, Deisseroth K, Kasparov S. Astrocytes control breathing through pH-dependent release of ATP. Science. 2010; 329:571–575. DOI: 10.1126/science.1190721 [PubMed: 20647426]

Honda H. Geometrical models for cells in tissues. Int Rev Cytol. 1983; 81:191–248. [PubMed: 6347934]

Hsiao HY, Chen YC, Huang CH, Chen CC, Hsu YH, Chen HM, Chiu FL, Kuo HC, Chang C, Chern Y. Aberrant astrocytes impair vascular reactivity in Huntington disease. Ann Neurol. 2015; 78:178–192. DOI: 10.1002/ana.24428 [PubMed: 25914140]

Humayun MS, Prince M, de Juan E, Barron Y, Moskowitz M, Klock IB, Milam AH. Morphometric analysis of the extramacular retina from postmortem eyes with retinitis pigmentosa. Invest Ophthalmol Vis Sci. 1999; 40:143–148. [PubMed: 9888437]

Iandiev I, Wurm A, Hollborn M, Wiedemann P, Grimm C, Remé CE, Reichenbach A, Pannicke T, Bringmann A. Müller cell response to blue light injury of the rat retina. Invest Ophthalmol Vis Sci. 2008; 49:3559–3567. DOI: 10.1167/iovs.08-1723 [PubMed: 18450590]

Jammalamadaka A, Suwannatat P, Fisher SK, Manjunath BS, Höllerer T, Luna G. Characterizing spatial distributions of astrocytes in the mammalian retina. Bioinformatics. 2015; 31:2024–2031. DOI: 10.1093/bioinformatics/btv097 [PubMed: 25686636]

Joeres S, Kirchhof B, Joussen AM. PVR as a complication of rhegmatogeneous retinal detachment: a solved problem? Br J Ophthalmol. 2006; 90:796–797. DOI: 10.1136/bjo.2005.088856 [PubMed: 16714271]

Ju WK, Kim KY, Noh YH, Hoshijima M, Lukas TJ, Ellisman MH, Weinreb RN, Perkins GA. Increased mitochondrial fission and volume density by blocking glutamate excitotoxicity protect glaucomatous optic nerve head astrocytes. Glia. 2015; 63:736–753. DOI: 10.1002/glia.22781 [PubMed: 25557093]

Karschin A, Wässle H, Schnitzer J. Immunocytochemical studies on astroglia of the cat retina under normal and pathological conditions. J Comp Neurol. 1986; 249:564–576. DOI: 10.1002/cne.902490410 [PubMed: 2427555]

Keeley PW, Reese BE. Morphology of dopaminergic amacrine cells in the mouse retina: independence from homotypic interactions. J Comp Neurol. 2010; 518:1220–1231. DOI: 10.1002/cne.22270 [PubMed: 20148440]

Kettenmann H, Verkhratsky A. Neuroglia: the 150 years after. Trends Neurosci. 2008; 31:653–659. DOI: 10.1016/j.tins.2008.09.003 [PubMed: 18945498]

Kinouchi R, Takeda M, Yang L, Wilhelmsson U, Lundkvist A, Pekny M, Chen DF. Robust neural integration from retinal transplants in mice deficient in GFAP and vimentin. Nat Neurosci. 2003; 6:863–868. DOI: 10.1038/nn1088 [PubMed: 12845328]

Kwon OW, Song JH, Roh MI. Retinal Detachment and Proliferative Vitreoretinopathy. Dev Ophthalmol. 2016; 55:154–162. DOI: 10.1159/000438972 [PubMed: 26501375]

Lesnik Oberstein SY, Lewis GP, Chapin EA, Fisher SK. Ganglion cell neurites in human idiopathic epiretinal membranes. Br J Ophthalmol. 2008; 92:981–985. DOI: 10.1136/bjo.2007.132332 [PubMed: 18577651]

Lewis, GP.; Fisher, SK. Plasticity in the Visual System, Retinal Plasticity and Interactive Cellular Remodeling in Retinal Detachment and Reattachment. Springer US; Boston, MA: 2006. Retinal Plasticity and Interactive Cellular Remodeling in Retinal Detachment and Reattachment; p. 55-78.

Lewis GP, Fisher SK. Up-regulation of glial fibrillary acidic protein in response to retinal injury: its potential role in glial remodeling and a comparison to vimentin expression. Int Rev Cytol. 2003; 230:263–290. [PubMed: 14692684]

Lewis GP, Linberg KA, Fisher SK. Neurite outgrowth from bipolar and horizontal cells after experimental retinal detachment. Invest Ophthalmol Vis Sci. 1998; 39:424–434. [PubMed: 9478003]

Lewis GP, Linberg KA, Geller SF, Guérin CJ, Fisher SK. Effects of the neurotrophin brain-derived neurotrophic factor in an experimental model of retinal detachment. Invest Ophthalmol Vis Sci. 1999; 40:1530–1544. [PubMed: 10359336]

Lewis GP, Matsumoto B, Fisher SK. Changes in the organization and expression of cytoskeletal proteins during retinal degeneration induced by retinal detachment. Invest Ophthalmol Vis Sci. 1995; 36:2404–2416. [PubMed: 7591630]

Linberg KA, Sakai T, Lewis GP, Fisher SK. Experimental retinal detachment in the cone-dominant ground squirrel retina: morphology and basic immunocytochemistry. Vis Neurosci. 2002; 19:603–619. [PubMed: 12507327]

Livet J, Weissman TA, Kang H, Draft RW, Lu J, Bennis RA, Sanes JR, Lichtman JW. Transgenic strategies for combinatorial expression of fluorescent proteins in the nervous system. Nature. 2007; 450:56–62. DOI: 10.1038/nature06293 [PubMed: 17972876]

Luna G, Lewis GP, Banna CD, Skalli O, Fisher SK. Expression profiles of nestin and synemin in reactive astrocytes and Müller cells following retinal injury: a comparison with glial fibrillar acidic protein and vimentin. Mol Vis. 2010; 16:2511–2523. [PubMed: 21139996]

Lye-Barthel M, Sun D, Jakobs TC. Morphology of astrocytes in a glaucomatous optic nerve. Invest Ophthalmol Vis Sci. 2013; 54:909–917. DOI: 10.1167/iovs.12-10109 [PubMed: 23322566]

Marc RE, Murry RF, Fisher SK, Linberg KA, Lewis GP. Amino acid signatures in the detached cat retina. Invest Ophthalmol Vis Sci. 1998; 39:1694–1702. [PubMed: 9699559]

Martone ME, Tran J, Wong WW, Sargis J, Fong L, Larson S, Lamont SP, Gupta A, Ellisman MH. The cell centered database project: an update on building community resources for managing and sharing 3D imaging data. J Struct Biol. 2008; 161:220–231. DOI: 10.1016/j.jsb.2007.10.003 [PubMed: 18054501]

Nakazawa T, Takeda M, Lewis GP, Cho KS, Jiao J, Wilhelmsson U, Fisher SK, Pekny M, Chen DF, Miller JW. Attenuated Glial Reactions and Photoreceptor Degeneration after Retinal Detachment in Mice Deficient in Glial Fibrillary Acidic Protein and Vimentin. Invest Ophthalmol Vis Sci. 2007; 48:2760–9. DOI: 10.1167/iovs.06-1398 [PubMed: 17525210]

Nguyen JV, Soto I, Kim KY, Bushong EA, Oglesby E, Valiente-Soriano FJ, Yang Z, Davis CHO, Bedont JL, Son JL, Wei JO, Buchman VL, Zack DJ, Vidal-Sanz M, Ellisman MH, Marsh-Armstrong N. Myelination transition zone astrocytes are constitutively phagocytic and have synuclein dependent reactivity in glaucoma. Proc Natl Acad Sci USA. 2011; 108:1176–1181. DOI: 10.1073/pnas.1013965108 [PubMed: 21199938]

Oberstein SYL, Byun J, Herrera D, Chapin EA, Fisher SK, Lewis GP. Cell proliferation in human epiretinal membranes: characterization of cell types and correlation with disease condition and duration. Mol Vis. 2011; 17:1794–1805. [PubMed: 21750605]

Ogata K, Kosaka T. Structural and quantitative analysis of astrocytes in the mouse hippocampus. Neuroscience. 2002; 113:221–233. [PubMed: 12123700]

Pearson-Leary J, Osborne DM, McNay EC. Role of Glia in Stress-Induced Enhancement and Impairment of Memory. Front Integr Neurosci. 2015; 9:63.doi: 10.3389/fnint.2015.00063 [PubMed: 26793072]

Pekny M, Pekna M. Astrocyte reactivity and reactive astrogliosis: costs and benefits. Physiol Rev. 2014; 94:1077–1098. DOI: 10.1152/physrev.00041.2013 [PubMed: 25287860]

Rattner A, Nathans J. An evolutionary perspective on the photoreceptor damage response. Am J Ophthalmol. 2006; 141:558–562. DOI: 10.1016/j.ajo.2005.10.045 [PubMed: 16490507]

Rattner A, Nathans J. The genomic response to retinal disease and injury: evidence for endothelin signaling from photoreceptors to glia. J Neurosci. 2005; 25:4540–4549. DOI: 10.1523/JNEUROSCI.0492-05.2005 [PubMed: 15872101]

Reese BE, Keeley PW. Design principles and developmental mechanisms underlying retinal mosaics. Biol Rev Camb Philos Soc. 2014; 90:854–876. DOI: 10.1111/brv.12139 [PubMed: 25109780]

Reichenbach A, Bringmann A. New functions of Müller cells. Glia. 2013; 61:651–678. DOI: 10.1002/glia.22477 [PubMed: 23440929]

Sakai T, Calderone JB, Lewis GP, Linberg KA, Fisher SK, Jacobs GH. Cone photoreceptor recovery after experimental detachment and reattachment: an immunocytochemical, morphological, and electrophysiological study. Invest Ophthalmol Vis Sci. 2003; 44:416–425. [PubMed: 12506104]

Senft SL, Woolsey TA. Mouse barrel cortex viewed as Dirichlet domains. Cereb Cortex. 1991; 1:348–363. [PubMed: 1822740]

Sethi CS, Lewis GP, Fisher SK, Leitner WP, Mann DL, Luthert PJ, Charteris DG. Glial remodeling and neural plasticity in human retinal detachment with proliferative vitreoretinopathy. Invest Ophthalmol Vis Sci. 2005; 46:329–342. DOI: 10.1167/iovs.03-0518 [PubMed: 15623793]

Smith SB, Brodjian S, Desai S, Sarthy V. Glial fibrillary acidic protein (GFAP) is synthesized in the early stages of the photoreceptor cell degeneration of the mivit/mivit (vitiligo) mouse. Exp Eye Res. 1997; 64:645–650. DOI: 10.1006/exer.1996.0249 [PubMed: 9227283]

Sofroniew MV. Molecular dissection of reactive astrogliosis and glial scar formation. Trends Neurosci. 2009; 32:638–647. DOI: 10.1016/j.tins.2009.08.002 [PubMed: 19782411]

Somjen GG. Nervenkitt: notes on the history of the concept of neuroglia. Glia. 1988; 1:2–9. DOI: 10.1002/glia.440010103 [PubMed: 2976736]

Son JL, Soto I, Oglesby E, Lopez-Roca T, Pease ME, Quigley HA, Marsh-Armstrong N. Glaucomatous optic nerve injury involves early astrocyte reactivity and late oligodendrocyte loss. Glia. 2010; 58:780–789. DOI: 10.1002/glia.20962 [PubMed: 20091782]

Srienc AI, Kornfield TE, Mishra A, Burian MA, Newman EA. Assessment of glial function in the in vivo retina. Methods Mol Biol. 2012; 814:499–514. DOI: 10.1007/978-1-61779-452-0_33 [PubMed: 22144328]

Stone, J. The whole mount handbook: a guide to the preparation and analysis of retinal whole mounts. 1981.

Strettoi E, Pignatelli V. Modifications of retinal neurons in a mouse model of retinitis pigmentosa. Proc Natl Acad Sci USA. 2000; 97:11020–11025. DOI: 10.1073/pnas.190291097 [PubMed: 10995468]

Strettoi E, Porciatti V, Falsini B, Pignatelli V, Rossi C. Morphological and functional abnormalities in the inner retina of the rd/rd mouse. J Neurosci. 2002; 22:5492–5504. [PubMed: 12097501]

Sun D, Jakobs TC. Structural remodeling of astrocytes in the injured CNS. Neuroscientist. 2012; 18:567–588. DOI: 10.1177/1073858411423441 [PubMed: 21982954]

Sun D, Lye-Barthel M, Masland RH, Jakobs TC. Structural remodeling of fibrous astrocytes after axonal injury. J Neurosci. 2010; 30:14008–14019. DOI: 10.1523/JNEUROSCI.3605-10.2010 [PubMed: 20962222]

Takahashi H, Kanesaki H, Igarashi T, Kameya S, Yamaki K, Mizota A, Kudo A, Miyagoe-Suzuki Y, Takeda S, Takahashi H. Reactive gliosis of astrocytes and Müller glial cells in retina of POMGnT1-deficient mice. Molecular and Cellular Neuroscience. 2011; 47:119–130. DOI: 10.1016/j.mcn.2011.03.006 [PubMed: 21447391]

Verardo MR, Lewis GP, Takeda M, Linberg KA, Byun J, Luna G, Wilhelmsson U, Pekny M, Chen DF, Fisher SK. Abnormal reactivity of muller cells after retinal detachment in mice deficient in GFAP and vimentin. Invest Ophthalmol Vis Sci. 2008; 49:3659–3665. DOI: 10.1167/iovs.07-1474 [PubMed: 18469190]

Vogler S, Pannicke T, Hollborn M, Grosche A, Busch S, Hoffmann S, Wiedemann P, Reichenbach A, Hammes HP, Bringmann A. Müller cell reactivity in response to photoreceptor degeneration in rats with defective polycystin-2. PLoS ONE. 2014; 8:e61631.doi: 10.1371/journal.pone.0061631 [PubMed: 23755094]

Wässle H, Peichl L, Boycott BB. Morphology and topography of on- and off-alpha cells in the cat retina. Proc R Soc Lond, B, Biol Sci. 1981; 212:157–175. [PubMed: 6166012]

Wilhelmsson U, Bushong EA, Price DL, Smarr BL, Phung V, Terada M, Ellisman MH, Pekny M. Redefining the concept of reactive astrocytes as cells that remain within their unique domains upon reaction to injury. Proc Natl Acad Sci USA. 2006; 103:17513–17518. DOI: 10.1073/pnas.0602841103 [PubMed: 17090684]

Zahs KR, Wu T. Confocal microscopic study of glial-vascular relationships in the retinas of pigmented rats. J Comp Neurol. 2001; 429:253–269. DOI: 10.1002/1096-9861(20000108)429:2<253::AID-CNE6>3.0.CO;2-S [PubMed: 11116218]

Zhang Y, Barres BA. Astrocyte heterogeneity: an underappreciated topic in neurobiology. Curr Opin Neurobiol. 2010; 20:588–594. DOI: 10.1016/j.conb.2010.06.005 [PubMed: 20655735]

Highlights

- Astrocytes are one of the least-well understood cell types in the retina, but our data indicates that they should now be included as a cell-type that can strongly react to photoreceptor degeneration.
- We used a combination of high-resolution immunostained mosaicked confocal images of whole mouse retina, single-cell injection, and comparative immunostaining data from several species to derive novel information about these cells in the normal and detached retina.
- Astrocytes in normal retina are often described as displaying a slender stellate appearance, the population is in fact heterogeneous with some cells showing tiled domains while others show significant overlap.
- After detachment astrocytes appear hypertrophic as their processes assume a thickened appearance and their endings appear less organized by anti-GFAP staining, but they largely remain within their anatomical domains, i.e. the cells do not generally grow larger.
- Significant structural remodeling in the detached retina includes the growth of processes deep into the retina along blood vessels, data not obvious in typical histological studies because of the very small size and relatively low number of astrocytes.

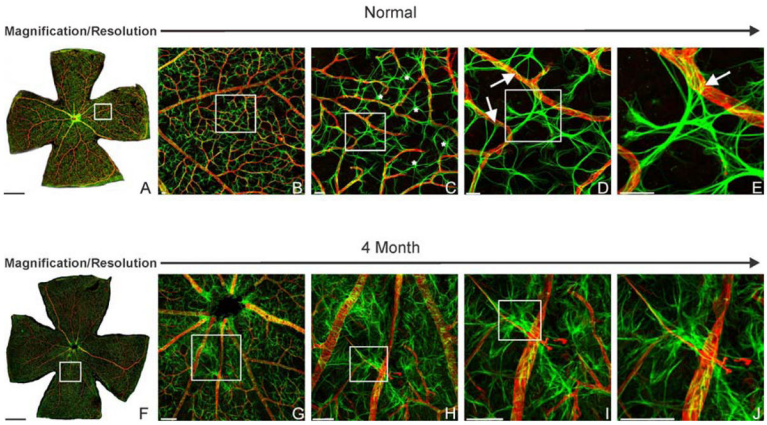

Figure 1.

Images from high-resolution montages using wholemounts of mouse retina stained with anti-GFAP (green, astrocytes), and anti-collagen type IV (red, blood vessels). **A–E**. Examples from a wholemount of normal retina. In the normal retina, processes of the smooth. Well-defined stellate-shaped (intravascular) astrocytes (examples marked by asterisks in A3) make discrete contacts (arrows, **D**, **E**) on blood vessels. **F–J**. Examples from a wholemount of a retina detached for 4 months. Sequential images in A–E and F–J show selected areas (white boxes) from the wholemounts in increasing magnification. After four months of retinal detachment astrocytes show dramatic changes in the GFAP staining. These cells lose their smooth stellate shape with their processes appearing “frayed” and making more branched and diffuse contacts with blood vessels. Scale bars = 200μm (A1, B1), 20μm (A2–5, B2–5).

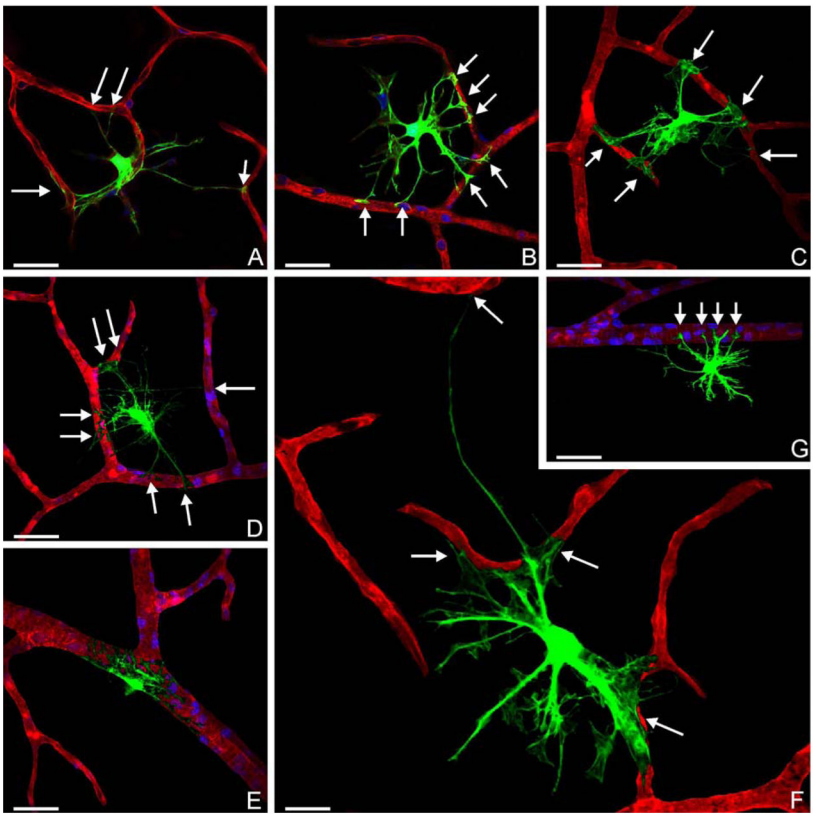

Figure 2.

Examples of individual astrocytes from normal mouse retina injected with the fluorescent dye Lucifer yellow (green). Blood vessels are stained with anti-collagen type IV (red). Arrows denote the contacts made by terminals of stellate intravascular astrocytes on blood vessles (**A–D**, **F**, **G**). A dye injected perivascular astrocyte whose soma directly apposes a blood vessel does not display the radial star-shaped morphology of the intravascular cells and appears to have an “ensheathing” relationship with its blood vessel (**E**). These perivascular astrocytes interact with only one blood vessel. Scale bars = 10μm.

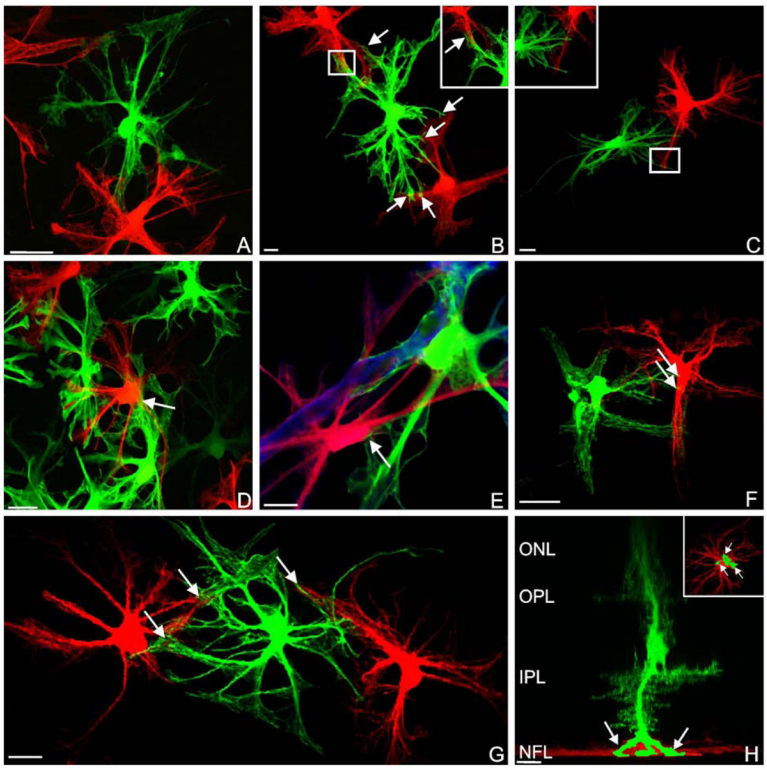

Figure 3.

Astrocytes from normal (**A–E**) and one month detached mouse retina (**F, G**) injected with two different fluorescent dyes, Lucifer yellow (green) and Alexa Fluor 568 (red). **A–C**. Examples of astrocytes with minimal to no overlap of their processes, i.e., tiled. However, these cells do appear to make discrete contacts with each other. Most intravascular astrocytes appear to be of this type. **D–E**. Perivascular astrocytes show a greater degree of overlap of their processes. In Figure E, blood vessels were labeled with PNA (blue). Both intravascular and perivascular astrocytes appear to form discrete contacts with each other (arrows). **F–G**. Intravascular astrocytes in a one month detached retina continue to maintain their tiled relationship and make discrete contacts (arrows) with each other. **H**. A dye-injected Muller cell (green; arrows) juxtaposed to a dye-injected astrocyte (red) showing the highly planar nature of astrocytes and the small degree of overlap between the endfeet of a Muller cell and the astrocyte. The inset shows a rotated view further emphasizing this small degree of overlap (arrows). Scale bars = 20μm.

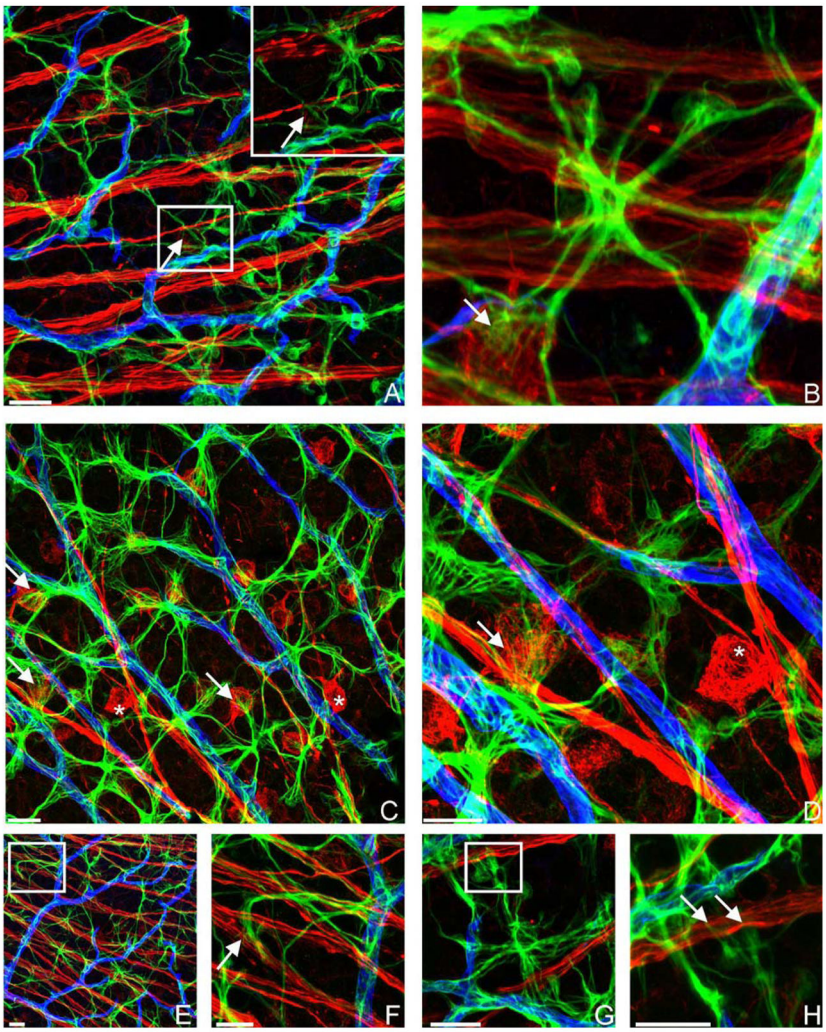

Figure 4.

A–D. Sampled regions in a normal mouse retinal wholemount displaying variability in the relationship between anti-GFAP labeled astrocytes (green), anti-SMI32 labeled ganglion cell bodies and their axons (red), as well as anti-collagen IV labeled blood vessels (blue). The arrows in A–C show ganglion cell bodies contacted by astrocytic terminals. The asterisks in C and D indicate ganglion cell bodies that appear to be neglected by astrocytic processes. **E–H**. Examples of astrocytic processes contacting ganglion cell axon bundles (arrows). F and H are higher magnifcation views of the boxed regions in E and G in which arrows indicate the interactions between astrocytic terminals and ganglion cell axons. Scale bars = 20μm.

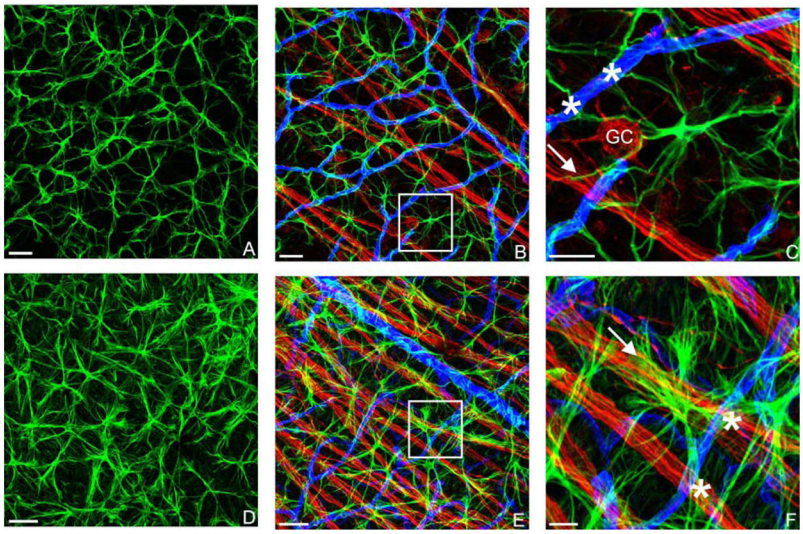

Figure 5.

A–F. Regions of normal (**A–C**) and four month detached mouse retina (**D–F**) labeled with anti-GFAP (astrocytes, green), anti-SMI32 (ganglion cell bodies and axons, red), and anti-collagen IV (blood vessels, blue). Figures A and D show the astrocytes alone demonstrating the structural changes in morphology after detachment. Figures B and E show data from all three channels demonstrating the interactions between other astrocytes, blood vessels, and ganglion cells. Figures C and F show the boxed areas in B and E at higher-magnification demonstrating that contacts between astrocytes, blood vessels and axons have a more diffuse and frayed appearance in the detached retina. Scale bars = 20μm.

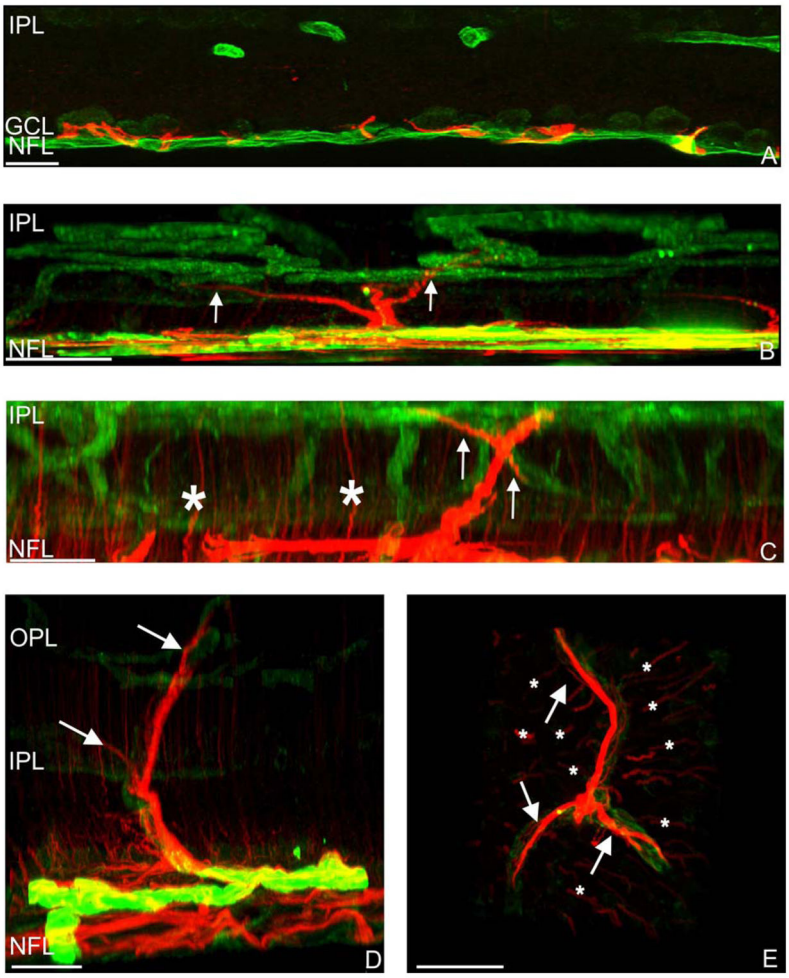

Figure 6.

Normal (**A**) and four month detached (**B–E**) mouse retina stained with anti-GFAP (red) and anti-collagen IV (green). **A**. In a 100 μm thick radial section, the thin highly planar nature of astrocytes within the GCL and nerve fiber layer (NFL) is obvious, demonstrating why the morphology of astrocytes is difficult to study in radially oriented sections of retina. **B–E**. Radial images across the retina generated by rotating specific areas selected from the wholemounts. By imaging selected astrocytes in a wholemount, rotating them and then reconstructing the cell in 3D we are more readily able to demonstrate the extent of remodeling of the cells by growth into the inner retina, and discriminate the thickened astrocyte process from the thinner GFAP-labeled Müller cells. **B**. After four months of induced detachment there is significant astrocytic remodeling indicated by the thickened branched process (red) following a blood vessel (green) into the inner plexiform layer (arrows). A second astrocyte process can be seen growing into the inner retina to the far right of the image. The intense yellow labeling in the NFL represents overlapping signals from staining of the superficial blood vessels and the increased anti-GFAP expression in astrocytes and Müller cell endfeet. **C**. A rotated view focused on the right ascending process of the astrocyte in the center of B, to more clearly show the thick nature of the process. The arrows indicate branches adjacent to blood vessels (green) in the inner retina. The gain in the

image was increased slightly to show the much finer anti-GFAP stained Müller cell processes (asterisks) traversing the inner retina. **D**. Occasionally astrocyte processes (red) grow as far as the outer plexiform layer (OPL). These also grow along blood vessels (green, arrows). **E**. A rotated view from a wholemount showing thick, remodeled processes of an astrocyte branching laterally in the IPL (arrows). The intense staining of the astrocyte processes almost obscures the fainter stained blood vessels to which they are closely apposed. This image also shows the thick nature of the remodeled astrocyte processes by comparison to the much finer Müller cell radial processes (asterisks). Scale bars = 20 μm.

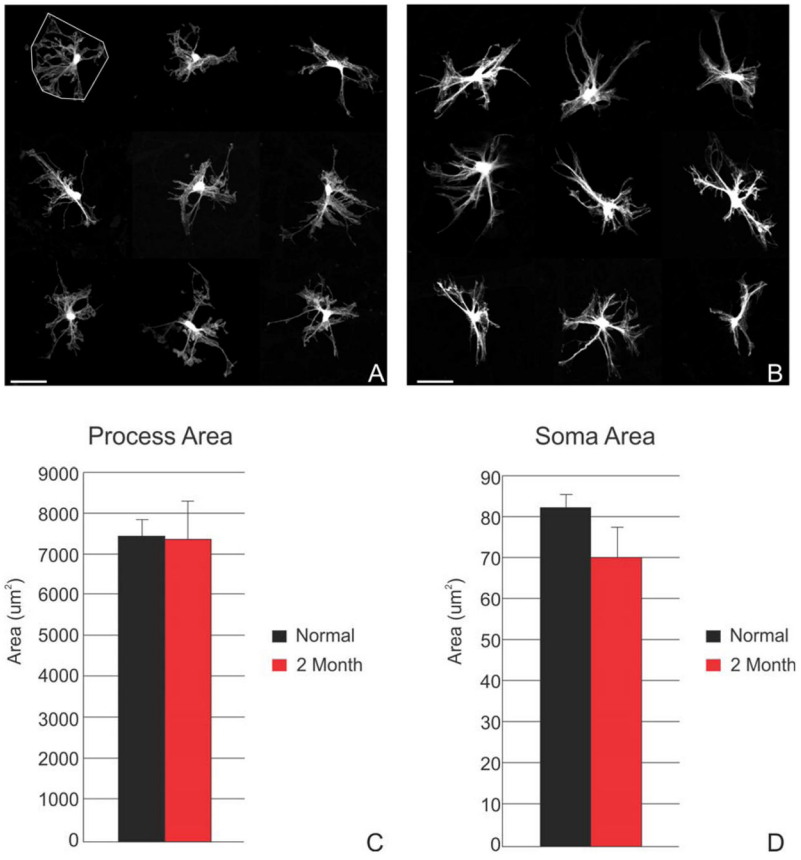

Figure 7.

A, **B**. Nine individual astrocytes from normal (**A**) and 2-month detached (**B**) mouse retina filled with the intracellular dye, Lucifer yellow. **C**, **D**. Data derived from these two data-sets demonstrate no significant differences between the area covered by the cellular processes, defined by a convex polygon as shown in A, or the apparent somal area of the cell. Error bars = standard deviation. Scale bars = 50μm.

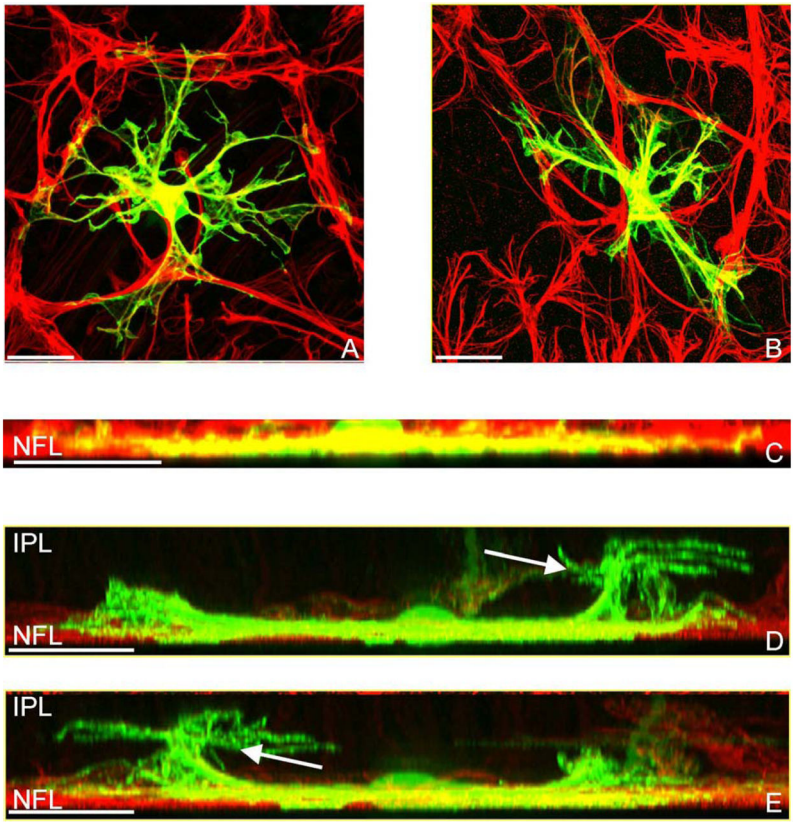

Figure 8.

Examples of Lucifer yellow injected intravascular astrocytes (green) in wholemounts also stained with anti-GFAP (red). **A**. Normal retina. **B–E**. Retina detached for 2 months. In normal retina the dye-filled cell shows the regular, fine processes that give the cell its "stellate" shape. With this particular cell, virtually all of its processes terminate on processes of other astrocytes. The reactive dye-filled astrocyte in B has more thickened processes and terminal endings that are more "blunt" with a "frayed" appearance by comparison to the cell in **A**. Notice that processes of the the anti-GFAP stained astrocytes (red) in B show similar characteristics. Overall thickening as well as growth into the inner retina is made more obvious by comparing the rotated views shown in figures **C–E**. The overlap of signals from anti-GFAP and Lucifer yellow are yellow, demonstrating that anti-GFAP gives an overall accurate, but incomplete image of astrocytes in both the normal and reactive states. **C**. Rotated higher magnification views of the astrocyte shown in **A**. Note the highly planar nature of the cell on the vitreal surface. **D**, **E**. Higher mangifcation rotated views at different angles of **B** showing the profusion of processes sprouting into the inner retina (**D, E**; arrows). Scale bars = 20 μm.

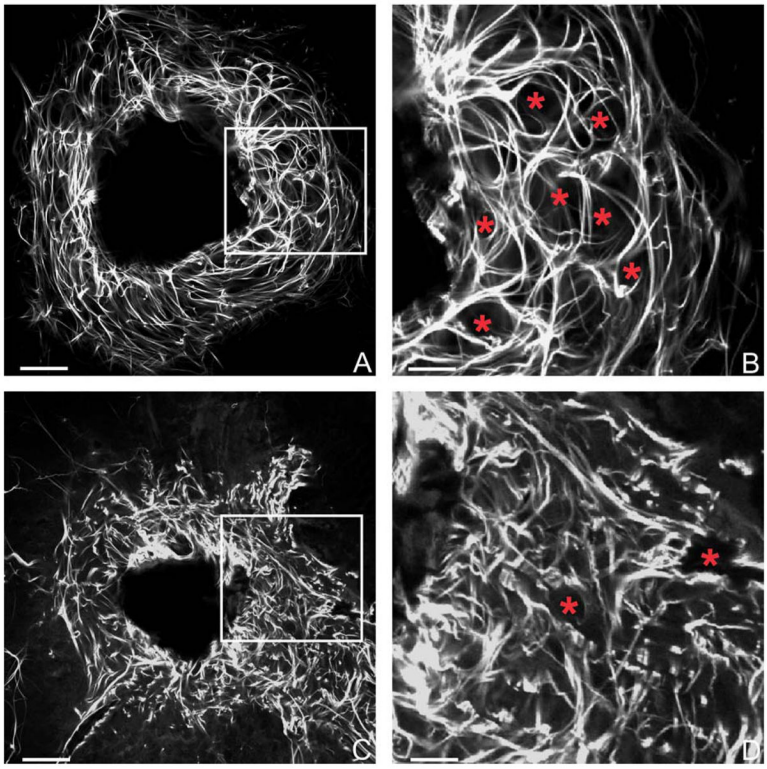

Figure 9.

Anti-GFAP stained optic nerve head (ONH) astrocytes in normal mouse (**A**, **B**) and 1 month detached mouse retina (**C**, **D**). In the detached retina the astrocytes appear thickened and disorganized by comparison to those in normal retina. **B**. A higher magnification image of the region within the white box in A demonstrates the well-defined glial openings (asterisks) which ganglion cell axon bundles traverse within the ONH. **D**. A higher magnification image of the the region within the white box in C shows both the hypertrophic appearance of these astrocytic processes, but the presence of far fewer organized glial openings (asterisks). Scale bar = 20μm.

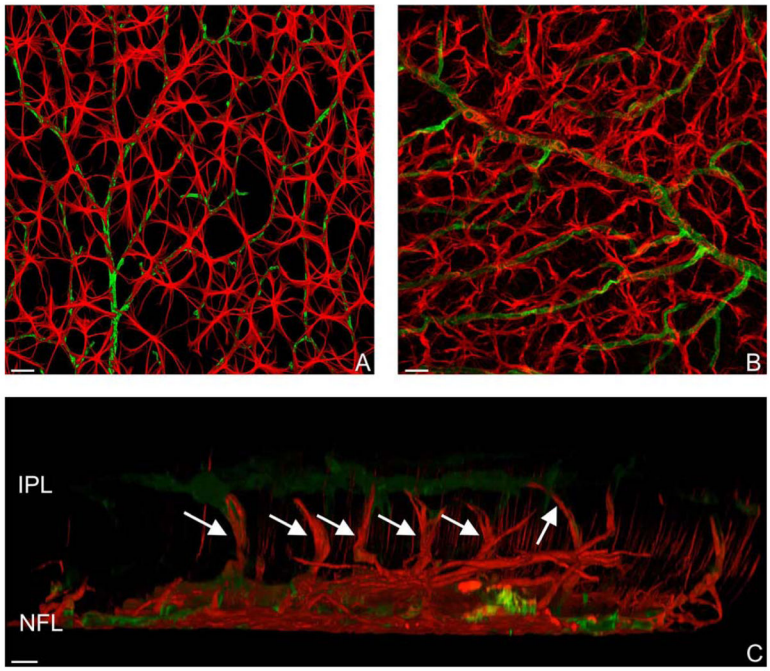

Figure 10.

A, **B**. A comparison of overall astrocyte morphology at P120 in a region of attached retina (A) and a region affected by a long-term detachment (B) in a mutant mouse showing the formation of serous-type retinal detachments. The intravascular astrocytes (red, anti-GFAP) show their classic slender, well-defined appearance with terminals that end on blood vessels (green, anti-collagen IV) and on other astrocytes. Astrocytes underlying an area of detachment are highly disorganized, with greatly thickened processes with a “ragged” morphology and poorly defined terminal endings on blood vessels. **C**. Anti-GFAP stained astrocytes in a region of detachment at P365 in the mutant mouse. The image has been selected from an area of astrocyte reactivity in a retinal wholemount and rotated by 90 degrees. There is extreme remodeling of astrocytes, with many thickened astrocyte processes growing into the inner plexiform layer (IPL; arrows). Note the thickness of these profiles relative to the Müller cell glial stalks that upregulate GFAP in this mutant mouse. As in the experimental rhegmatogenous detachments, astrocyte processes growing into the inner retina associate with blood vessels in detachments caused by the mutation. Scale bars = 20μm.

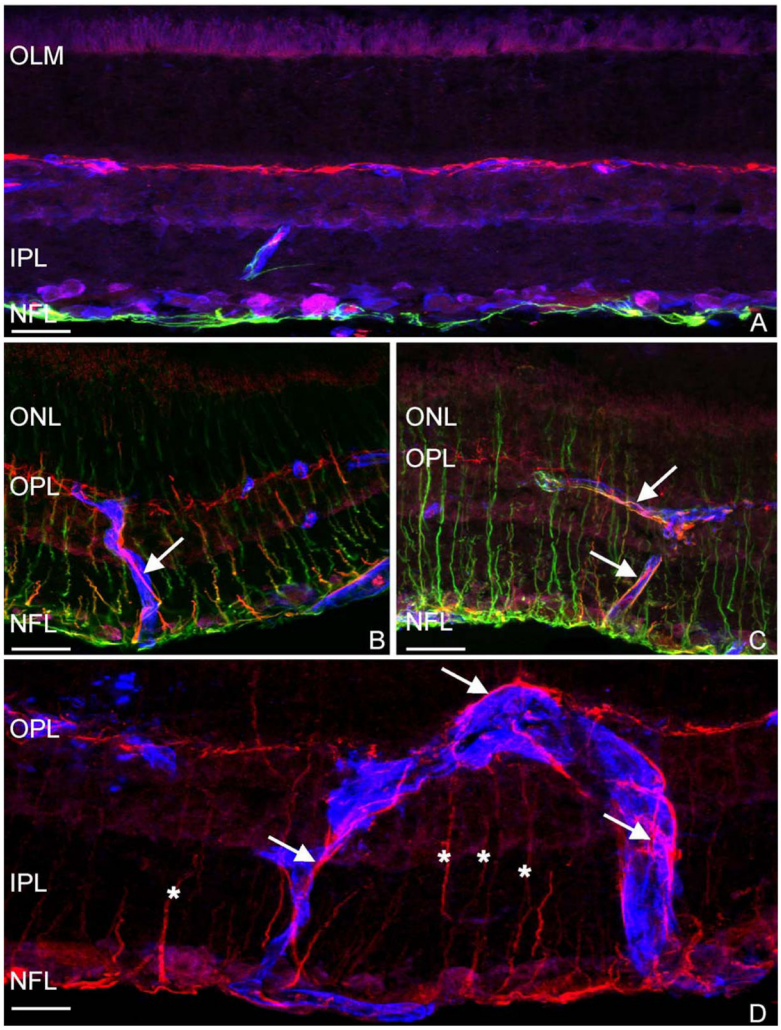

Figure 11.

The responses of astrocytes in a rat model of rhegmatogenous retinal detachment. **A**. A radial section of a normal rat retina stained with isolectin B4 (blue, blood vessels), anti-GFAP (green, astrocytes), and anti-synemin (red). The astrocytes have a typical planar morphology forming a thin layer along the vitreal surface of the retina, and do not label with anti-synemin. (The red shown in "A" is background labeling.) **B**, **C**, **D**. After one month of detachment astrocytes up-regulate their expression of synemin and extend processes into the inner retina along blood vessels (arrows). Reproduced from Luna et al., 2010. Scale bars = 20μm.

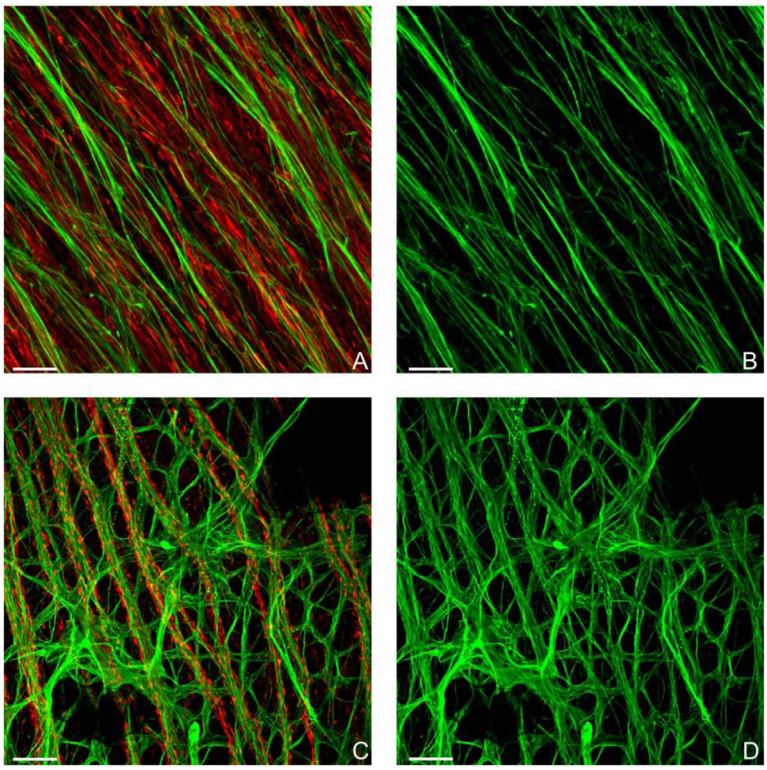

Figure 12.

Images from wholemounts of human retina stained with anti-GFAP (green) and anti-neurofilament (red). **A**, **B**. In normal retina astrocyte processes travel along the bundles of ganglion cell axons on the vitreal surface. The regular, long, slender appearance of these processes are better appreciated in the absence of the red channel (B). **C**, **D**. Examples of astrocyte morphology in a human retina affected by age-related macular degeneration and stained with anti-GFAP (green) and anti-neurofilament (red). The astrocytes show a highly disorganized appearance with many processes running at angles to the axon bundles. Also note the more beaded appearance of the axons. Only the anti-GFAP channel is shown in D. Scale bars = 20μm.

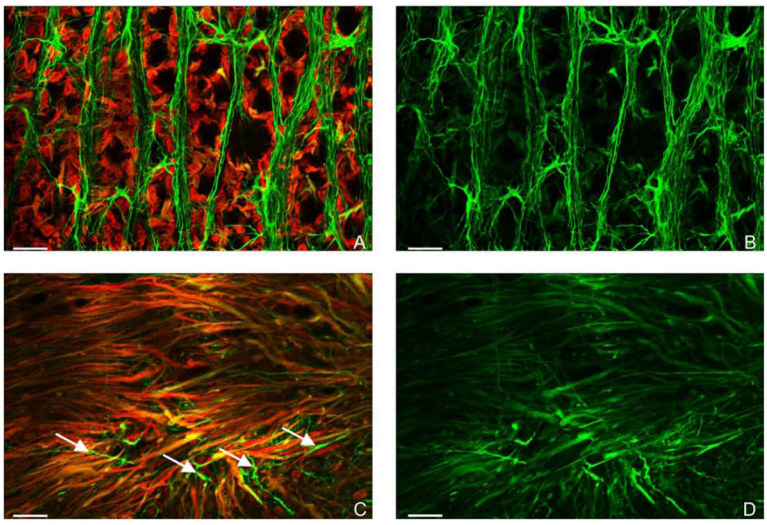

Figure 13.

Images of feline retina stained with anti-GFAP (green) and anti-vimentin (red). **A**. In the normal cat retina, Müller cell endfeet label predominately with anti-vimentin but also slightly with anti-GFAP, hence their orange hue; their endfeet form regular arrays around the ganglion cells. **A**, **B**. Astrocytes label only with anti-GFAP and their processes follow bundles of ganglion cell axons in an orderly manner. **C**. After seven days of retinal detachment Müller cell endfeet grow chaotically on the retinal surface and label with both anti-vimentin and anti-GFAP giving them more of an orange/yellow appearance. **C**, **D**. Astrocyte processes (green) still label exclusively with anti-GFAP and intermingle in a disorganized fashion with Müller cell processes on the retinal surface. B and D are the same images as in A and C, respectively, with only the GFAP labeling shown. Scale bars = 20μm. A and C reproduced from (Lewis and Fisher, 2006).

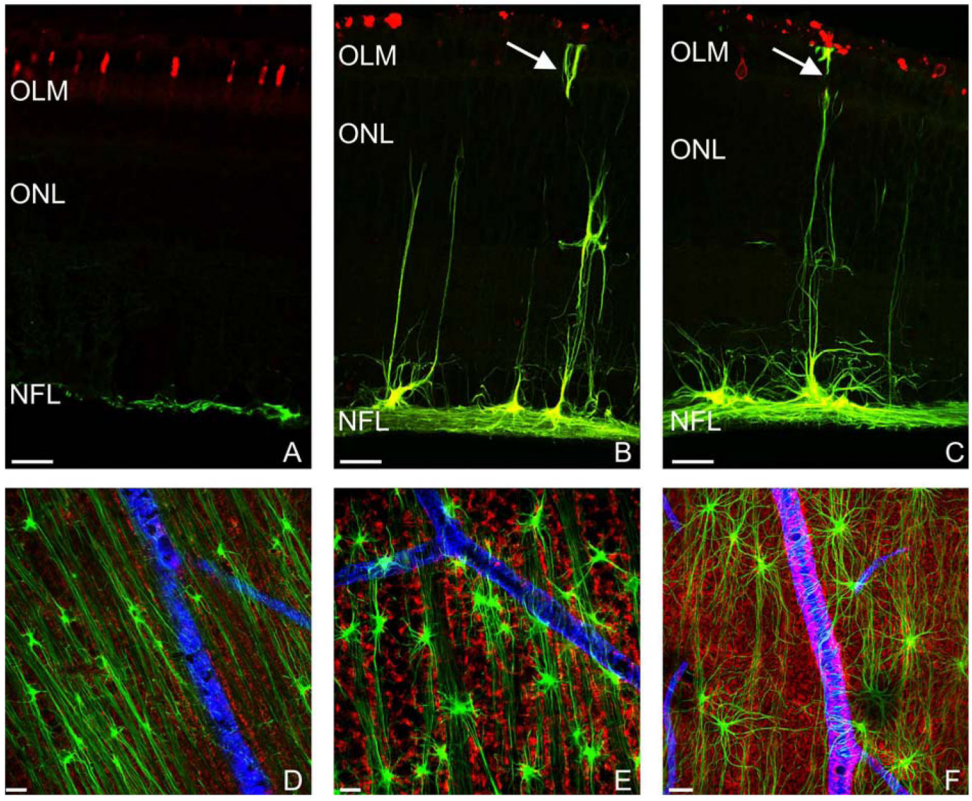

Figure 14.

Examples of astrocyte reactivity in the California ground squirrel retina. **A–C**. Examples of astrocyte staining in normal squirrel retina and a retina that was detached for 1 day and reattached for 3 weeks. Staining with anti-M-cone opsin shows the location of the photoreceptor outer segment layer. **A**. In normal retina the astrocytes, as in all other species, are confined to the NFL. **B**, **C**. In the reattached retina astrocyte remodeling is extensive and prominently different than in all other species with a profusion of GFAP-positive processes growing into the inner and outer retina, in some instances reaching the outer limiting membrane (OLM). Note that there is almost no staining of Müller cells in either the normal or detached retinas in this species. **D**,**E**,**F**. Examples from wholemounted ground squirrel retina stained with anti-GFAP (green), anti-vimentin (red), and anti-collagen IV (blue). **D**. In the normal retina, astrocytes (green) display an appearance similar to the cat retina, with their processes forming linear tracks along ganglion cell axons. Müller cell endfeet stain lightly with anti-vimentin (red). Note that there are few recognizable terminals of astrocytes on the BV. **E.** After 1 day of detachment and 3 weeks of reattachment astrocytes begin to assume a more disorganized appearance and the Müller endfeet begin to thicken and stain more robustly with anti-vimentin (red). **F**. Following 1 day of detachment and 3 months of reattachment, the astrocytes show a loss of their linear orientation along the ganglion cell axon bundles and assume a highly stellate appearance, with processes radiating in all directions. Unlike in other species reactive Müller cells do not appear to upregulate their expression of anti-GFAP in response to detachment. They do however appear to become more profusely branched with a less organized array of endfeet on the vitreal surface (F). In this species, Müller cell reactivity includes much more coverage of the retinal blood vessels

(blue) by their endfeet (F, pink). A, B, and C were modified from Sakai et al., 2003. Scale bars = 20μm.